

## Research Paper

# Rationale for Fixed Dosing of Pertuzumab in Cancer Patients Based on Population Pharmacokinetic Analysis

Chee M. Ng,<sup>1,4</sup> Bert L. Lum,<sup>1</sup> Veronica Gimenez,<sup>2</sup> Steve Kelsey,<sup>3</sup> and David Allison<sup>1</sup>

Received October 4, 2005; accepted February 8, 2006

**Objective.** Our objectives were to develop the population pharmacokinetic (PK) for pertuzumab and examine the variability of steady-state trough serum concentrations ( $C_{SS, \text{trough}}$ ) and exposure after fixed, body-weight-based, or body-surface area (BSA)-based dosing methods in cancer patients.

**Methods.** Pertuzumab was administered by IV infusion (every 3 weeks) either as a weight-based dose (0.5–15 mg/kg) or a fixed dose (420 or 1050 mg). Data from three clinical studies, comprising 153 patients and 1458 concentration-time points, were pooled for this analysis using NONMEM.

**Results.** A linear two-compartment model best described the data. Body weight and BSA were significant covariates affecting clearance (CL) and distribution volume (Vc), respectively. However, weight and BSA only explained small percentage of interpatient variability for CL and Vc, respectively. Simulation results indicated that PK profiles were very similar after the three dosing methods. Compared to fixed dosing, weight- and BSA-based dosing only reduced the population variability of  $C_{SS, \text{trough}}$  moderately.

**Conclusion.** A population PK model was developed for pertuzumab, the first monoclonal IgG1 antibody in a new class of agents known as HER dimerization inhibitors. In addition, our analyses demonstrate the feasibility of administering pertuzumab using a fixed dose in women with ovarian and breast cancers.

**KEY WORDS:** cancer; fixed dosing; human epidermal growth factor receptors; monoclonal antibody; population pharmacokinetics.

## INTRODUCTION

Human epidermal growth factor receptors (HER/ErbB) interact to form ligand-activated homo- and heterodimers, which are implicated in the proliferation and survival of many solid tumors. Pertuzumab (also known as recombinant human monoclonal antibody 2C4; Omnitarg™, Genentech, Inc., South San Francisco, CA, USA) represents the first in a new class of agents known as HER dimerization inhibitors (HDI) and functions to inhibit the ability of HER2 to form active heterodimers with other HER receptors (such as EGFR/HER1, HER3, and HER4) and is active irrespective of HER2 expression levels (1–4). Pertuzumab blockade of the formation of HER2–HER3 heterodimers in tumor cells has been demonstrated to inhibit critical cell signaling, which results in reduced tumor proliferation and survival (5). The pertuzumab binding site does not overlap with the epitope on HER-2 that is recognized by trastuzumab (Herceptin®; Genentech Inc.) (4). In addition, the mechanism of action

of pertuzumab is distinct from tyrosine kinase inhibitors such as gefitinib or erlotinib that bind competitively to the intracellular adenosine triphosphate binding site of HER receptors (6).

Pertuzumab has undergone testing as a single agent in the clinic with a phase Ia trial in patients with advanced cancers and phase II trials in patients with ovarian cancer and breast cancer as well as lung and prostate cancers. In a phase Ia study, patients with incurable, locally advanced, recurrent, or metastatic solid tumors that had progressed during or after standard therapy were treated with pertuzumab given intravenously every 3 weeks. Pertuzumab was generally well tolerated. Tumor regression was achieved in 3 of 20 patients evaluable for response. Two patients had confirmed partial responses. Stable disease lasting for more than 2.5 months was observed in 6 of 21 patients (7). At doses of 2.0–15 mg/kg, the pharmacokinetics of pertuzumab was linear, and mean clearance ranged from 2.69 to 3.74 mL/day/kg and the mean terminal elimination half-life ranged from 15.3 to 27.6 days. Antibodies to pertuzumab were not detected (7,8). Pertuzumab was dosed on a weight basis (mg/kg) in this phase I trial, and following pharmacokinetic (PK) analysis and simulation study, phase II trials were initiated using a fixed dose (9). Typically, commercially available human IgG monoclonal antibodies [i.e., trastuzumab, bevacizumab, and rituximab (Genentech Inc.), and gemtuzumab ozogomicin (Wyeth Pharmaceuticals, Philadelphia, PA)] and cytotoxic small molecule drugs in oncology have been administered on a

<sup>1</sup>Department of Pharmacokinetic and Pharmacodynamic Sciences, Genentech Inc., 1 DNA Way MS70, South San Francisco, California 94080-4990, USA.

<sup>2</sup>Department of Oncology, Hoffman-La Roche, Basel, Switzerland.

<sup>3</sup>Department of BioOncology, Genentech Inc., South San Francisco, California 94080-4990, USA.

<sup>4</sup>To whom correspondence should be addressed. (e-mail: cheeng@gene.com)

weight-based (mg/kg) or body surface area-based (BSA) dosing method. Historically, this was a result of the practice legacy of initiation of clinical studies based on species scale-up and animal toxicity data (10). However, in a recent retrospective assessment of 33 investigational anticancer drugs in 1650 patients, in only five drugs was BSA-based dosing thought to be of clinical relevance (11). A recent review on marketed anticancer drugs further suggested that proper scientific rationale for BSA-based dosing of anticancer drugs in adults is lacking, and fixed dosing strategies should be implemented (12). Although the relevance of BSA- and weight-based dosing for small molecule anticancer agents has been recognized and examined, its significance has not been fully appreciated and remains unstudied for most monoclonal antibodies in oncology.

This is the first reported population PK analysis of pertuzumab, first monoclonal IgG1 antibody that inhibits HER dimerization, and is, to our knowledge, the first critical assessment of the impact and utility of fixed dosing of a human IgG1 monoclonal antibody on pharmacokinetics and target drug concentrations. The primary objectives of this analysis of pertuzumab were to (1) evaluate the population PK and predictive covariates for pertuzumab in cancer patients and (2) examine the variability of steady-state trough concentrations and exposures after fixed or body-weight- and BSA-based dosing.

## METHODS

### Studies and Patients

All three studies used in this analysis were approved by the appropriate ethics committees of the participating centers. Written informed consent was obtained from all patients before entry onto study.

Study 1 was a phase Ia, open-label, multicenter, dose-escalation study to evaluate the safety, tolerability, and PK profiles of pertuzumab administered intravenously as a single agent to subjects with advanced solid malignancies. These patients received a dose of pertuzumab administered by the IV route every 3 weeks as a 90-min IV infusion on the first cycle and then as a 30-min infusion in subsequent cycles. Doses were escalated (0.5, 2, 5, 10, and 15 mg/kg) in cohorts of three or six subjects until the maximum tolerated dose (MTD) was defined or the highest dose level was reached. During the first cycle of treatment, serum samples for determination of pertuzumab concentrations were collected at serial time points: prior to the dose, at the end of the IV infusion, at 1.5, 4, and 9 h, and on days 2, 5, 8, and 15. During the second treatment cycle, serum samples for determination of pertuzumab concentrations were collected prior to the dose, 29 min following the start of the IV infusion, and on day 8.

Study 2 was a phase II, open-label, single-arm, multicenter trial to evaluate the overall efficacy, safety, tolerability, and the effect of tumor-based HER2 activation on the efficacy of pertuzumab in patients with advanced ovarian cancer, in which their disease was refractory to or had recurred following prior chemotherapy. These women received IV infusions of pertuzumab administered as a single agent over a 90-min period during the first cycle of treatment at a fixed dose of 840

mg, followed by a 420-mg maintenance dose, delivered as a 30-min infusion every 3 weeks during subsequent treatment cycles. During the first and second treatment cycle, serum samples for determination of pertuzumab concentrations were collected prior to the dose, 15 min following the end of the infusion, and at days 8 and 15. Additional serum samples for determination of pertuzumab concentrations were collected prior to the dose and 15 min after the end of the IV infusion during subsequent treatment cycles.

Study 3 was a phase II, open label, single-arm, multicenter randomized study to evaluate the efficacy and safety of two different doses of pertuzumab administered as a single agent in patients with metastatic breast cancer with low expression of HER2. In the first dose cohort, patients received pertuzumab as an IV infusion administered over a 90-min period as an 840-mg loading dose on the first cycle, followed by a maintenance dose of 420 mg given every 3 weeks as a 30-min IV infusion during subsequent treatment cycles. In the second dose cohort, the patients received an IV infusion of pertuzumab as a 1050-mg dose over a 90-min period on the first cycle and as a 1050-mg dose as a 30-min IV infusion every 3 weeks during subsequent treatment cycles. In study 3, serum samples for determination of pertuzumab concentrations were collected prior to the dose, 15 min following the end of infusion, and on days 8 and 15 during the first two treatment cycles. Additional serum samples for determination of pertuzumab concentrations were collected prior to the dose and 15 min after the end of infusion during subsequent treatment cycles.

### Drug Assay

Pertuzumab serum concentrations were determined by a validated receptor-binding, enzyme-linked immunosorbent assay. The assay used p185HER2 extracellular domain to capture pertuzumab from serum samples. Bound pertuzumab was detected with mouse antihuman Fc-horseradish peroxidase (Jackson ImmunoResearch Laboratories, Inc., West Grove, PA, USA), and tetramethyl benzidine (KPL, Inc., Gaithersburg, MD, USA) was used as the substrate for color development to quantify serum pertuzumab. The assay has a minimum quantifiable concentration of 0.25 µg/mL for pertuzumab in human serum.

### Population Pharmacokinetic Analysis

Population nonlinear mixed-effect modeling was performed using NONMEM (13) software (Version V, Level 1.0) with NM-TRAN and PREDPP and the Compaq Visual Fortran compiler (Version 6.5). Two different basic structural models, a one- and two-compartmental linear PK model with IV infusion, were fit to serum pertuzumab concentration-time data. The first-order conditional estimation (FOCE) method with interaction between inter- and intraindividual variability was used throughout the model-building procedure. An exponential error model was used to describe the interindividual variability for the PK parameters. A multiplicative covariate regression model was implemented as follows:

$$\hat{P}_i = \theta_1 \left( \frac{X_i}{\text{med}(X)} \right)^{\theta_x} \quad (1)$$

**Table I.** Demographic Characteristics of the Patients Included in the Analysis

	Median	Range
Age (years)	56	32–78
BSA* (m <sup>2</sup> )	1.73	1.40–2.53
Weight (kg)	69.0	45.0–150.6
Albumin (g/L)	39.2	21.0–52.0
Alkaline phosphatase (ALK) (IU/L)	107.0	39.0–367.0
	Number of patients	Percentage
Gender		
Male	8	5.2
Female	145	94.8
Race		
Caucasian	141	92.2
African American	3	2.0
Hispanic	4	2.6
Asian	3	2.0
Native Indian	0	0
Others	2	1.3

\*BSA = body surface area.

where the  $\theta_x$  is the regression coefficient to be estimated for continuous [e.g., body weight (WT)]. Continuous variables  $X_i$  were centered on their median [ $\text{med}(X_i)$ ] values, thus allowing  $\theta_1$  to represent the clearance estimate for the typical patient with median covariates. The residual variability was modeled as proportional-additive error model.

The relationships between structural model-based Bayesian estimates of the PK parameters and individual covariates were explored graphically. Based on preliminary exploratory analyses, the effect of each covariate on PK parameters was tested. Comparison of alternative structural models and construction of the covariate model was based on the typical goodness-of-fit diagnostic plots and likelihood ratio test. When comparing alternative models, the differences in the value of the objective function are approximately chi-square-distributed with  $n$  degrees of freedom ( $n$  is the difference in the number of parameters between the full and the reduced model). This approximation has been shown to be reliable for the FOCE-INTERACTION estimation method (14). To discriminate two nested models and select significant covariates, a difference in an objective function of greater than 7.9 (1 degree of freedom), which corresponds to a significance level of  $p < 0.005$ , was used.

The fraction of interindividual variance (% variance) explained by the covariates in the regression model for given PK parameters [e.g., clearance (CL)] was computed as follows:

$$\% \text{ variance} = \left( \frac{\omega_{\text{CL,BASE}}^2 - \omega_{\text{CL,FINAL}}^2}{\omega_{\text{CL,BASE}}^2} \right) \times 100 \quad (2)$$

where  $\omega_{\text{CL,BASE}}^2$  and  $\omega_{\text{CL,FINAL}}^2$  represented interindividual variance of clearance in base and final PK model, respectively.

## Population Pharmacokinetic Model Evaluation

The model evaluation in this study utilized a bootstrap resampling technique to evaluate the stability of the final model and estimate the confidence interval of parameters. This model evaluation technique consists of first creating data sets using the bootstrap option in the software package Wings for NONMEM (N Holford, Version 404, June 2003, Auckland, New Zealand) and then obtaining parameter estimates for each of the replicate data sets. The results from 1000 successful runs were obtained, and the mean and 2.5th and 97.5th percentiles (denoting the 95% confidence interval) for the population parameters were determined and compared with the estimates of the original data.

In addition, *a posteriori* predictive model checks were used to evaluate the ability of the final model to describe the observed data (15–17). In these analyses, the 2.5th, 5th, 10th, 25th, 50th (median), 75th, 90th, and 95th percentiles of the observed data were computed and selected as the test statistics for the posterior predictive model check. The final

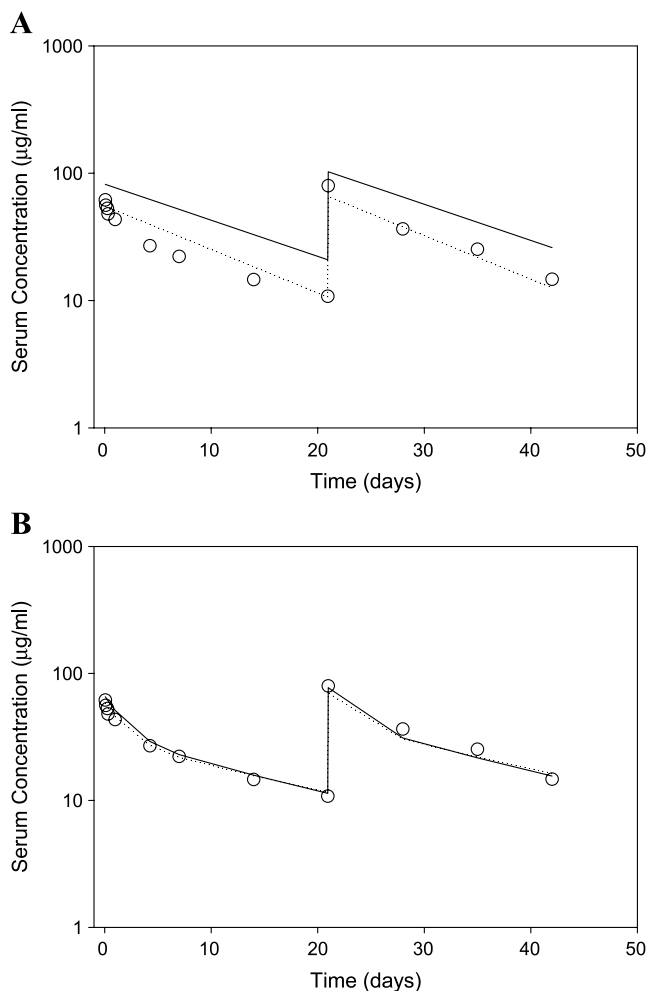


**Fig. 1.** Representative profile of a single subject's pharmacokinetic (PK) data fitted by a one- (A) or two- (B) compartmental model. Open circle indicates observed concentration. Solid and dotted lines indicate population predicted and individual predicted concentration, respectively.

population PK model, including final fixed and random-effect parameters, was used to simulate 1000 replicates of the observed data set, and test statistics were computed from each of those simulated data set. The posterior predictive distribution of test statistics from the simulated data set was then compared with the observed test statistics, and the  $p$  value ( $p^{\text{PPC}}$ ) can be estimated by calculating the proportion of cases in which test statistics from the simulated data set exceed or is below the realized value of observed test statistics according to the following (16):

$$p^{\text{PPC}} = \frac{1}{N} \sum_{i=1}^{1000} I(T(y_i^{\text{rep}}, \theta) > \text{or} < T(y, \theta_i)) \quad (3)$$

where  $I(\cdot)$  is the indicator function that takes the value 1 when its argument is true and 0 otherwise.  $T(y, \theta)$  is a “realized value” of the observed test statistics because it is realized by the observed data  $y$ .  $T(y_i^{\text{rep}}, \theta)$  is the test statistics from a simulated data set  $i$  (range from 1 to 1000) (16). A  $p$  value of less than 0.05 or greater than 0.95 would indicate that the observed test statistics were significantly different from the posterior distribution of the test statistics in the simulated data set, and the model did not adequately describe the observed data. In addition, the 2.5th, 5th, 95th, and 97.5th quantiles of the simulated data were calculated for each time points for individual patients. The numbers of observed data that fell within the boundaries of the 2.5th and 95.5th quantiles (95% interval), and 5th and 95th quantiles (90% interval) of the pooled simulated data were determined.

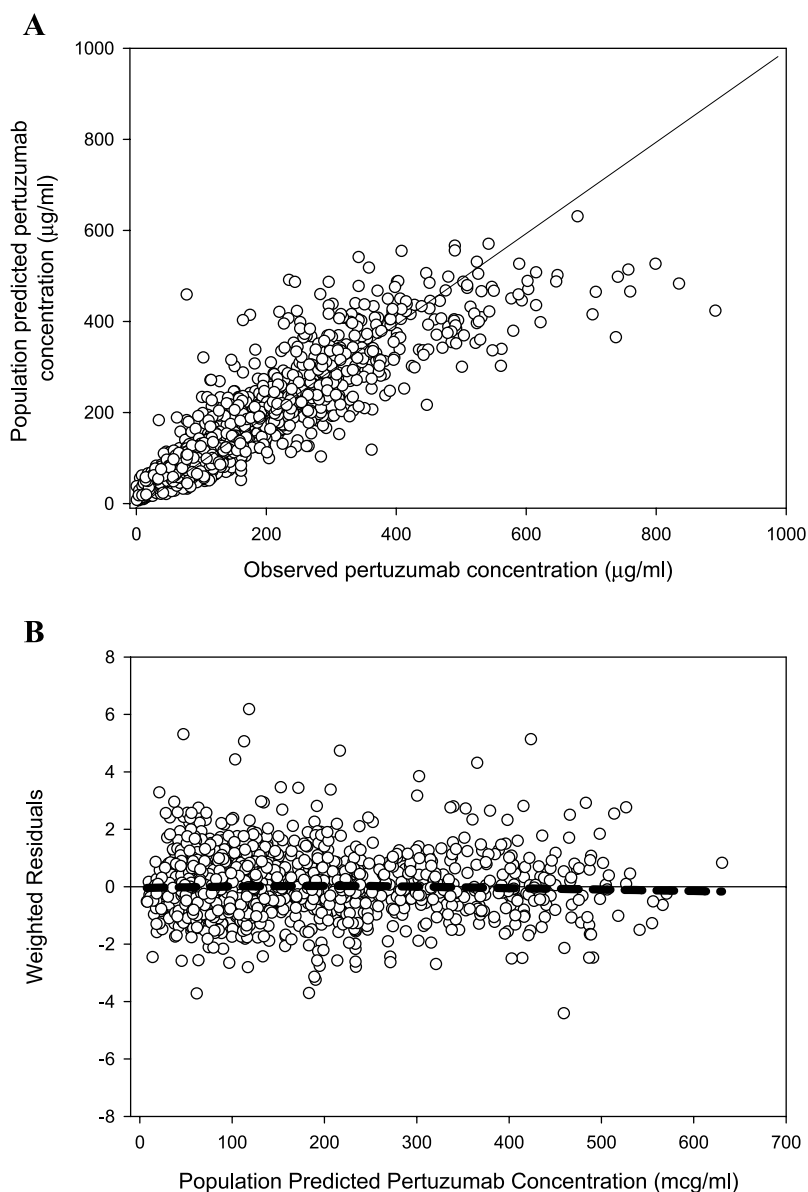


**Fig. 2.** Model diagnostic plots. (A) Observed vs. predicted pertuzumab concentrations. The solid line is the line of unity. (B) Weighted residuals vs. predicted pertuzumab concentrations. The dashed line is a LOESS smooth of data.

### Pertuzumab Exposures after Fixed, BSA-, and Weight-Based Dosing

The final population PK model was used to determine the serum pertuzumab concentration-time profiles and steady-state trough concentrations and exposure after fixed, BSA-, and weight-based dosing. Serum concentration-time profiles and clearance of pertuzumab for 1000 subjects were simulated for a fixed, BSA-based, or weight-based dosing regimen using the final model with a data set obtained by bootstrapping (with replacement) the original PK data set. All simulated subjects received an 840-mg, 12.2-mg/kg, or 485-mg/m<sup>2</sup> IV infusion over 90 min on day 0, then a 420-mg, 6.1-mg/kg, or 242.5-mg/m<sup>2</sup> IV infusion over 30 min on days 21, 42, and 63. Steady-state trough concentrations obtained on day 84 ( $C_{SS, \text{trough}}$ ) after different dosing regimens were then assessed. In addition, the percent of subjects with steady-state trough concentrations below a target concentration (20 µg/mL) after a fixed, BSA-based, or weight-based dose were calculated. Simulated clearance values were used to determine the steady-state average exposure ( $AUC_{SS0-\tau}$ ) according to:

$$AUC_{SS0-\tau} = \frac{\text{Dose}}{CL} \quad (4)$$

where  $\tau$  is the dosing interval of pertuzumab.

## RESULTS

### Demographic Data

The demographic characteristics of the patients included in this PK analysis are listed in Table I. A total of 1458 pertuzumab serum concentration time points were collected from 153 patients in the three studies. Of the total, 18 patients were from the phase Ia trial, 60 from the phase II ovarian cancer trial, and 75 from the phase II breast cancer trial. Thus, the majority (94.8%) of the patients in this analysis were female and accounted for 1110 (76%) of the serum pertuzumab concentration data. All subjects had low HER2 expression tumor confirmed by fluorescence *in situ* hybridization analysis and had good physical functional status as indicated by an Eastern Cooperative Oncology Group performance status of either 0 or 1. The number of patients with missing covariates was very low (4.6% for both height and BSA), and the missing covariates were imputed with the median values. In 384 (20.8%) serum pertuzumab concentration samples with only a documented sampling date, the sampling time was imputed to occur at 12 noon. An analysis was conducted by removing the concentrations with imputed sampling time to assess the effects of these data on the population parameter estimates in the model, and this revealed no significant influence (data not shown).

### Population PK Analysis

A two-compartment model described the data better than one-compartment model based on the change of objective function ( $\delta = -736.2$ ) and diagnostic plots. A representative pertuzumab serum concentration-time profile fit to a one- and

two-compartment model is illustrated in Fig. 1. Compared to two-compartment model, a three-compartment model did not improve the fit significantly ( $\delta = -5.05$ ,  $df = 2$ ,  $p > 0.05$ ) with the parameter K13 estimated poorly (%CV > 1000). Therefore, two-compartment linear PK model was selected as the final structural model. The interindividual variability term ( $\eta$ ) for the distribution rate constant from central to peripheral compartment (K12) was removed from two-compartmental models because the removal of this  $\eta$  term did not result in a statistically significant increase ( $\delta < 7.88$ ) in the objective function. In an exploratory analysis using the final base model, no apparent relationships between potential covariates and  $\eta_{K21}$  were identified. Therefore, only covariate effects on  $\eta_{CL}$  and  $\eta_{Vc}$  were examined during the development of the final model with covariates.

For the final model with covariates, predicted vs. observed pertuzumab serum concentrations and weighted residuals vs. predicted serum concentration plots are shown in Fig. 2. In the final model, serum albumin (ALB), body weight (BW), and serum alkaline phosphatase (ALKP) were the most significant covariates explaining interindividual variability for pertuzumab clearance (CL). BSA was the most significant covariate explaining interindividual variability of pertuzumab central compartment volume of distribution ( $V_c$ ). Incorporation of covariance terms among  $\eta_{CL}$ ,  $\eta_{Vc}$ , and  $\eta_{K21}$  using full OMEGA BLOCK improved the fit ( $\delta = -14.0$ ,  $df = 3$ ). However, the estimated correlation was not large ( $r_{CL-Vc} = 0.45$ ;  $r_{CL-K21} = 0.28$ ;  $r_{Vc-K21} = 0.39$ ), and the parameter estimates were not influenced (data not shown). In addition, majority (67%) of the runs using the model with

**Table II.** Parameter Estimates of the Final Population Pharmacokinetic Model and the Stability of the Parameters Using a Bootstrap Validation Procedure

	Original data set Estimate (%RSE) <sup>a</sup>	1000 Bootstrap replicates Mean (95% CI)
<b>Structural model</b>		
CL (L/day)	0.214 (3.1)	0.214 (0.201, 0.228)
V <sub>c</sub> (L)	2.740 (1.9)	2.739 (2.640, 2.840)
K <sub>12</sub> (day <sup>-1</sup> )	0.203 (16.6)	0.220 (0.159, 0.416)
K <sub>21</sub> (day <sup>-1</sup> )	0.258 (15.6)	0.275 (0.203, 0.480)
<b>Interindividual variability</b>		
CL %CV	31.1 (11.0)	30.6 (27.0, 34.1)
V <sub>c</sub> %CV	16.2 (20.3)	16.0 (12.7, 19.2)
K <sub>21</sub> %CV	25.2 (37.6)	24.1 (11.4, 33.6)
<b>Covariate model</b>		
ALB on CL ( $\theta_{ALB, CL}$ )	-1.010 (18.4)	-1.019 (-1.420, -0.632)
WT on CL ( $\theta_{WT, CL}$ )	0.587 (19.3)	0.589 (0.372, 0.826)
ALKP on CL ( $\theta_{ALKP, Vc}$ )	0.169 (29.5)	0.170 (0.067, 0.258)
BSA on V <sub>c</sub> ( $\theta_{BSA, Vc}$ )	1.160 (12.2)	1.151 (0.890, 1.451)
<b>Residual variability</b>		
Proportional error $\sigma_{prop}^2$	0.037 (19.4)	0.037 (0.030, 0.045)
Additive error, $\sigma_{prop}$ (µg/mL)	2.265 (77.8)	2.24 (0.002, 4.160)

<sup>a</sup> %RSE: percent relative standard error of the estimate = SE/parameter estimate × 100.

covariance terms failed to minimize successfully in the 1200 bootstrap runs (>90%). Furthermore, both models (with or without covariance terms) produced very similar results in the posterior model checks (data not shown). These results indicated that model incorporating the covariance terms with full OMEGA BLOCK was not stable and does not improve the predictability of the model. Hence, the model without the covariance terms in the OMEGA BLOCK was selected as the final model and illustrated as follows:

$$\text{CL} = \theta_{\text{CL}} \times \left(\frac{\text{WT}}{69}\right)^{\theta_{\text{WT-CL}}} \times \left(\frac{\text{ALB}}{39.2}\right)^{\theta_{\text{ALB-CL}}} \times \left(\frac{\text{ALKP}}{107}\right)^{\theta_{\text{ALKP-CL}}} \quad (5)$$

$$\text{Vc} = \theta_{\text{Vc}} \times \left(\frac{\text{BSA}}{1.72}\right)^{\theta_{\text{BSA-Vc}}} \quad (6)$$

The parameter estimates of the final model are summarized in Table II. The CL of serum pertuzumab in the analysis population was estimated to be 0.214 L/day and the Vc was 2.74 L. The  $K_{12}$  and  $K_{21}$  were 0.203 and 0.258 day<sup>-1</sup>, respectively. Interindividual variability for CL and Vc in the

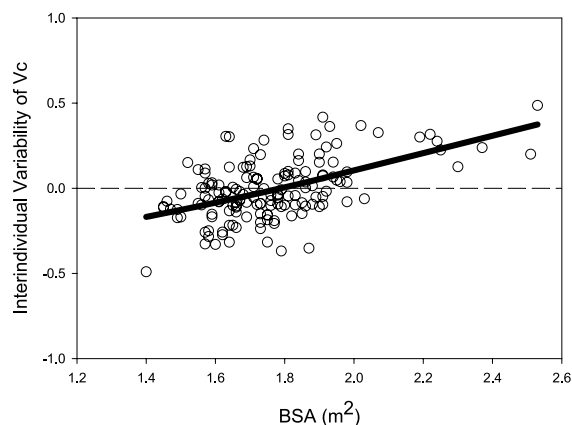
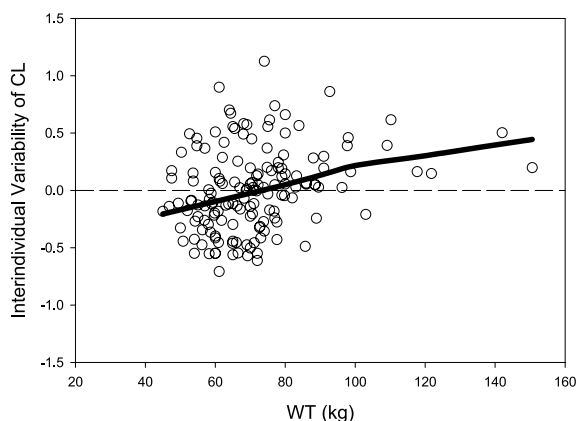
final model, calculated as the square root of interindividual variance ( $\omega^2$ ) and expressed as %CV, are 31.1 and 16.2%, respectively, compared to 38.0 and 20.8% for the base model without covariates. The covariate effect of ALB, WT, and ALKP in the final model therefore explained about 33% of the interindividual variance for CL. However, weight alone explained only 8.3% of interpatient variability for CL. The covariate effect of BSA explained about 39% of interindividual variance for Vc in the final model. The dependency of CL on WT and Vc on BSA with the base model is accounted for in the final model as shown in Fig. 3. The estimated distribution and elimination half-life ( $t_{1/2\alpha}$  and  $t_{1/2\beta}$ ) were 1.4 and 17.2 days, respectively.

### Model Evaluation

From the original data set, 1000 successful bootstrap runs were obtained and compared to the original observed data. Mean population PK estimates obtained from the bootstrap procedure were similar to the parameter estimates of the original data set (Table II), indicating that the developed model was stable. The 95% confidence intervals for the fixed-effect parameters were narrow, which indicated good precision.

A *posteriori* predictive model check was used to evaluate the ability of the final model to describe the observed data.

### A Base Model



### B Final Model

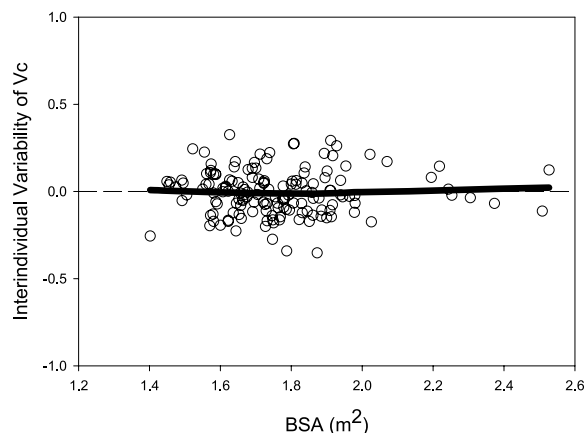
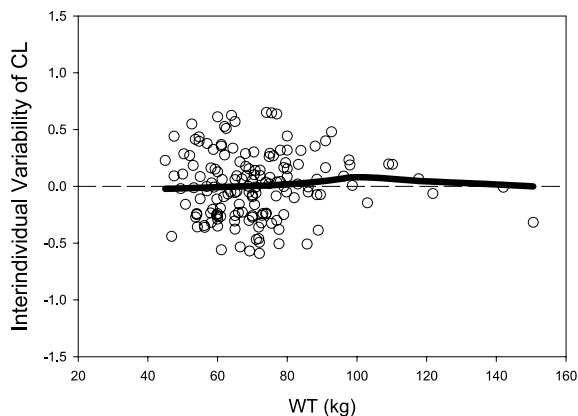


**Fig. 3.** Random effect ( $\eta$ ) for clearance (CL) by weight (WT) and Vc by body-surface area (BSA) for the (A) base model and (B) final model.

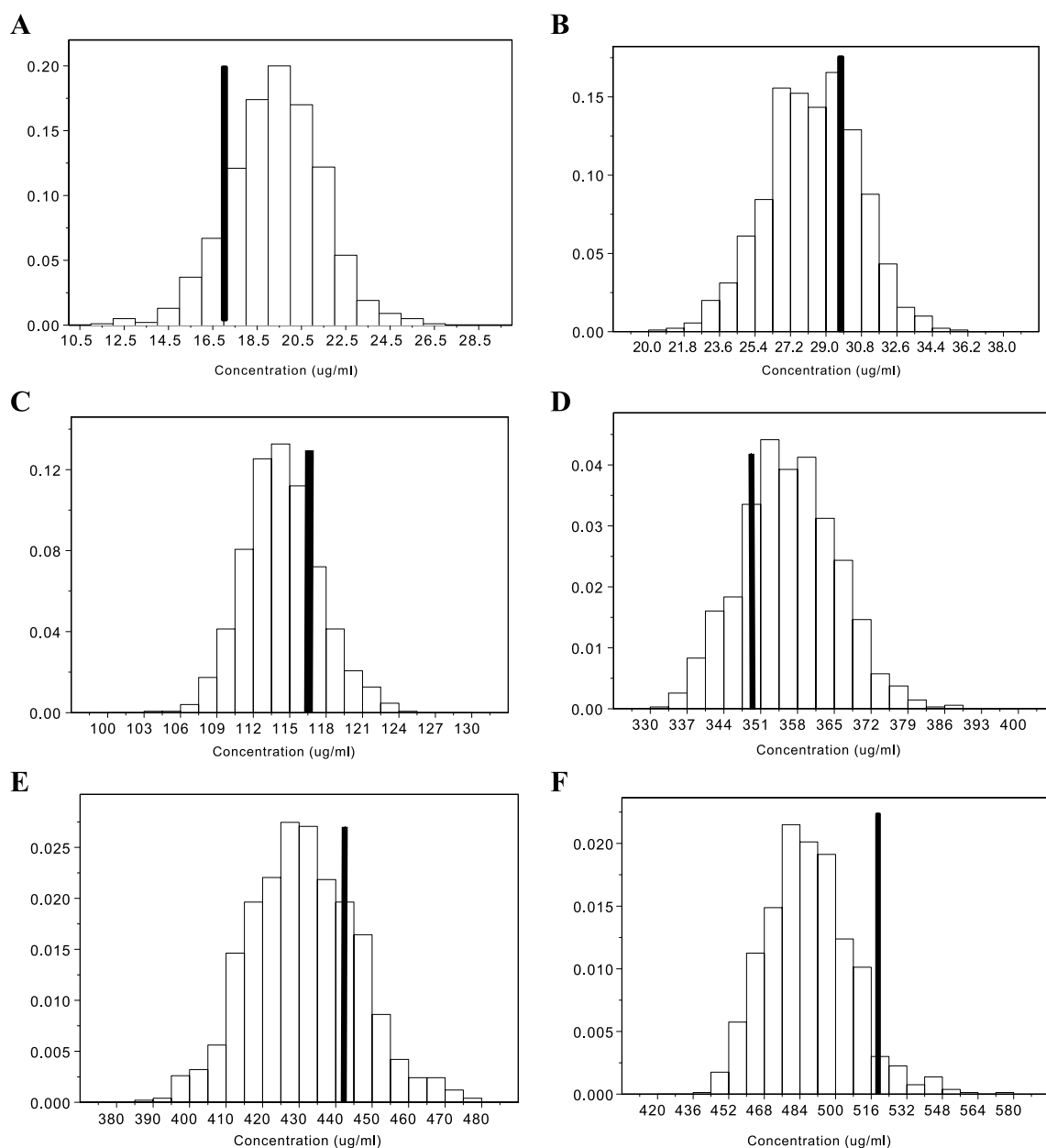


**Fig. 4.** Model evaluation of pertuzumab final population PK model using a posterior model check. Posterior predictive distribution and observed values for the test statistics: (A) 2.5th; (B) 5th; (C) 50th; (D) 90th; (E) 95th; (F) 97.5th. The vertical line on each histogram represents the observed value of the test statistic.

The final population PK model, including final fixed and random-effect parameters, was used to simulate 1000 replicates. The test statistics were then computed for each of those 1000 simulated data sets. Figure 4 displays histograms of the 1000 simulated values of selected test statistics, with the “realized value” of the observed test statistics indicated by vertical line. The posterior predictive distributions were close to the observed values with the estimated  $p$  values between 0.05 and 0.95 for each test statistic. In addition, the percentages of observed pertuzumab concentrations within 90 and 95% quantile range of the pooled simulated data were 89.3 and 94.7%, respectively. These results suggested that the model was able to describe and predict the data reasonably well.

#### **Pertuzumab Exposures after Fixed, BSA-, and Weight-Based Dosing**

Predicted serum pertuzumab concentration-time profiles and steady-state trough concentrations on day 84 ( $C_{SS, \text{trough}}$ ) were estimated for 1000 simulated subjects bootstrapped from the original PK data set and the final model using a fixed, weight-based, or BSA-based dose according to the dose schedules outlined in Methods. The simulated serum pertuzumab concentration-time profiles after a fixed, weight-based, or BSA-based dose were very similar and consistently above the targeted serum concentrations of 20  $\mu\text{g/mL}$  (Fig. 5). For weight-based and BSA-based dosing, population variability of  $C_{SS, \text{trough}}$  decreased by 6.17 and 5.76%, respectively, when

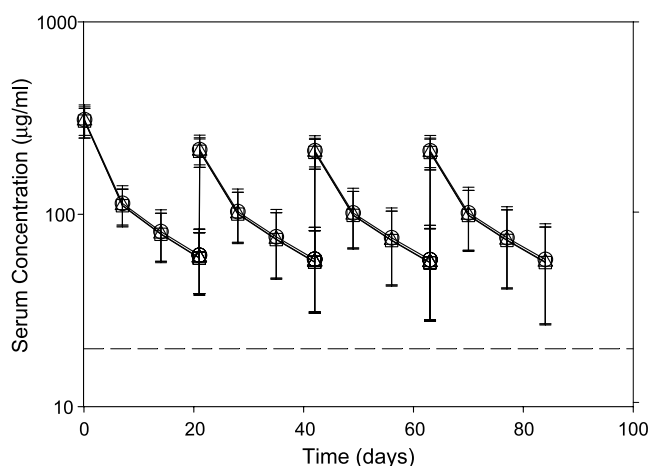


**Fig. 5.** Simulated serum pertuzumab concentration-time profiles (mean  $\pm$  SD) following fixed (circle), WT (square), and BSA-based (triangle) dosing regimens. Dashed line: set targeted serum pertuzumab concentration of 20  $\mu\text{g/mL}$ .

compared to fixed dosing (Fig. 6 and Table III). The percentages of subjects with  $C_{SS, \text{trough}}$  below a target serum concentration of 20  $\mu\text{g/mL}$  were similar, with values of 8.3, 8.7, and 8.3% for fixed, weight-based, or BSA-based dosing, respectively (Table III). Similar results were obtained from the analysis of pertuzumab serum steady-state  $\text{AUC}_{\text{SS}0-\tau}$  for 1000 simulated subjects, and weight- and BSA-based dosing only reduced the population variability by 2.2 and 4.2%, respectively, when compared to fixed dosing. The same simulated data set was used to determine  $C_{SS, \text{trough}}$  after a fixed dose, weight-, and BSA-based dose for populations with extreme weight (i.e.,  $\text{WT} \leq 10\text{th}$  and  $\geq 90\text{th}$  percentile; Fig. 7). Median pertuzumab  $C_{SS, \text{trough}}$  for population with WT less than or equal to 10th percentile were 72.3 (range 8.7–166.5), 52.8 (range 6.8–125.7), and 63.2 (range 7.8–150.1)  $\mu\text{g/mL}$  for a fixed dose, weight-, and BSA-based dose, respectively. The percentages of subjects in population with  $C_{SS, \text{trough}}$  below a

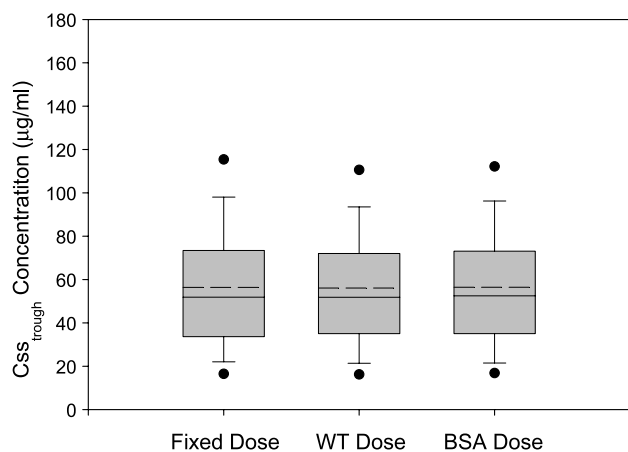


**Fig. 6.** Predicted pertuzumab steady-state trough concentration (day 84) after a fixed, WT-, or BSA-based dose for 1000 simulated subjects bootstrapped from original PK data set according to the final model.

**Table III.** Predicted Pertuzumab Steady-State Trough Concentration (Day 84) After a Fixed, Weight-, or BSA-Based Dose for 1000 Simulated Subjects Bootstrapped from Original Pharmacokinetic Data Set According to the Final Model

	$C_{SS, \text{trough}}$ ( $\mu\text{g/mL}$ ), fixed dose	$C_{SS, \text{trough}}$ ( $\mu\text{g/mL}$ ), weight-based dose	$C_{SS, \text{trough}}$ ( $\mu\text{g/mL}$ ), BSA-based dose
Minimum	2.68	2.39	2.54
5th percentile	16.56	16.32	16.86
Median	51.87	51.81	52.48
Mean	56.37	56.08	56.44
95th percentile	115.38	110.46	112.14
Maximum	209.67	179.06	192.00
%CV	54.05	52.62	52.40
Variance	928.21	870.93	874.71
% Variance changed from fixed dose <sup>a</sup>	–	–6.17	–5.76
Percent of subjects with $C_{SS, \text{trough}} \leq 20 \mu\text{g/mL}$	8.3	8.7	8.3

<sup>a</sup>Percent variance changed from fixed dose was calculated using the following equation: Percent variance change =  $\frac{\text{Variance}_{\text{WT or BSA-based dose}} - \text{Variance}_{\text{fixed dose}}}{\text{Variance}_{\text{fixed dose}}} \times 100$ .

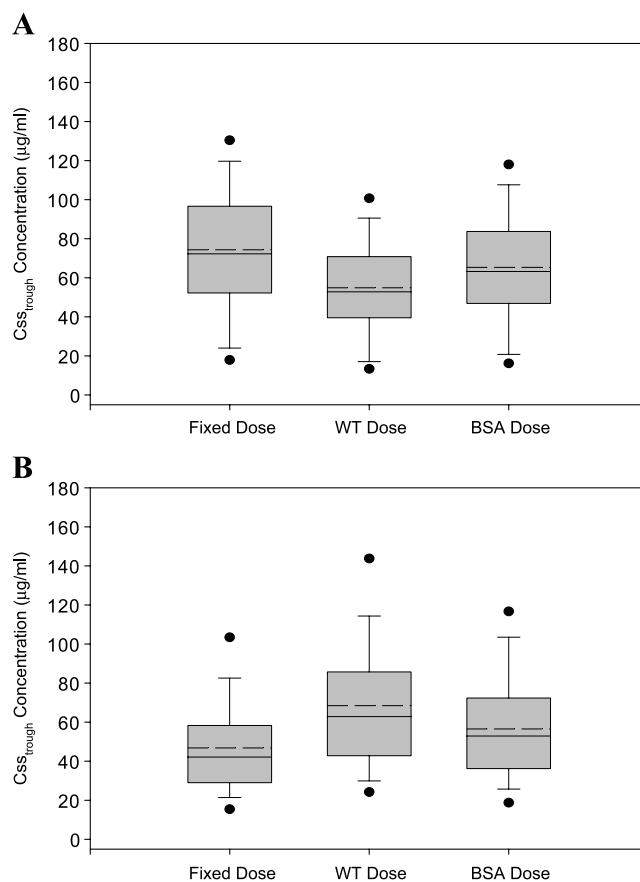


**Fig. 7.** Predicted pertuzumab steady-state trough concentration (day 84) after a fixed, WT-, or BSA-based dose for patient populations with (A)  $\leq 10\text{th}$  (50.4 kg) or (B)  $\geq 90\text{th}$  (88.5 kg) WT values.



target serum concentration of 20  $\mu\text{g/mL}$  were 5.4, 12.6, and 9.0% for fixed, weight-based, and BSA-based dosing, respectively. Median pertuzumab  $C_{\text{SS},\text{trough}}$  for population with WT greater than or equal to 90th percentile were 42.1 (range 7.0–119.8), 62.8 (range 14.4–167.3), and 52.9 (range 10.2–133.3)  $\mu\text{g/mL}$  for a fixed dose, weight-, and BSA-based dose, respectively. The percentages of subjects in this population with  $C_{\text{SS},\text{trough}}$  below a target serum concentration of 20  $\mu\text{g/mL}$  were similar, with values of 7.4, 2.8, and 5.6% for fixed, weight-based, or BSA-based dosing, respectively. Similar results were obtained for the analysis of pertuzumab serum steady state  $\text{AUC}_{\text{C}_{\text{SS}0-\tau}}$  of these subgroups from 1000 simulated subjects (data not shown).

## DISCUSSION

Pertuzumab is a humanized monoclonal IgG1 antibody that inhibits tumor growth and survival by a novel mechanism of action—inhibition of HER-2 dimerization with other ligand-activated HER kinases. Pertuzumab has undergone testing in the clinic with a phase Ia trial in patients with advanced cancers and in phase II trials in patients with ovarian, breast, lung, and prostate cancers. Pertuzumab was dosed on a weight basis (mg/kg) in the phase Ia trial and as a fixed dose in phase II trials. Using demographic and serum pertuzumab concentration-time data collected in these three trials, we were able to build a first population PK model with predictive covariates for pertuzumab PK in cancer patients. Typically, human IgG monoclonal antibodies and cytotoxic small molecule drugs in oncology have been administered on a weight-based (mg/kg) or BSA-based dose basis. Using the final model and simulation, we are able to provide a rationale for the fixed dosing of pertuzumab in cancer patients with potential broad application to other IgG1 monoclonal antibody and proteins.

Pertuzumab PK obtained from this analysis was very similar to those reported for other human monoclonal IgG1 drugs used in oncology (18–20). A linear two-compartment PK model best described the data, and in the final model, pertuzumab CL was 0.214 L/day. Typical Vc of pertuzumab was 2.74 L or approximately 40 mL/kg, which is equal to human plasma volume and was consistent with values reported for other monoclonal IgG1 drugs (18,20). Pertuzumab CL was significantly affected by body weight and serum concentrations of albumin and alkaline phosphatase, whereas Vc was significantly influenced by BSA. The effect of sex on pertuzumab PK could not be assessed because of the small number of male subjects (5.2%) included in the analysis. The lack of relationships between the pertuzumab PK and age implied that no dosage adjustment is necessary based on age alone in patients up to 78 years old. The results from a bootstrap procedure and posterior model checking suggested that the final model was stable and able to describe and predict the data reasonably well.

The effect of weight on CL and BSA on Vc suggested that pertuzumab might be dosed based on either body weight or BSA. However, the covariate effect of weight alone and BSA alone in the model only explained about 8.3 and 40% of the interindividual effect of CL and Vc, respectively. This suggested that although weight is a predictor of CL and BSA is a predictor of Vc, the effect of weight and BSA on pertuzumab

exposures after dosing might be measurable but not highly contributory.

Therefore, our next step was to assess the impact of the various dosing methods on the pertuzumab exposures using simulations. In dose-response studies, using a preclinical tumor xenograft mouse model showed that >80% suppression of growth for various tumor types is achieved at steady-state trough concentrations of approximately 5–25  $\mu\text{g/mL}$  (21), suggesting that the efficacy of the pertuzumab may be related to steady-state trough concentrations. In a phase Ia study, there is no apparent relationship between toxicity and administered doses ranged from 0.5 to 15 mg/kg given intravenously every 3 weeks (7). Two patients, one with ovarian cancer (5 mg/kg) and one with pancreatic islet cell carcinoma (15 mg/kg), achieved a partial clinical response, suggesting that pertuzumab dose of at least 5 mg/kg administered every 3 weeks may be related to clinical response. In this study, pertuzumab infusion given at doses greater than 5 mg/kg every 3 weeks ensured that serum concentration remains above 20  $\mu\text{g/mL}$ . Pertuzumab was well tolerated, and an MTD (at doses up to 15 mg/kg) was not reached in this study. The PK parameter estimates were very similar for dose group 2–15 mg/kg, suggesting that PK parameters alone were unlikely related to clinical response/toxicity as long as the desirable therapeutic concentrations were achieved. Therefore, based on the findings from this phase Ia clinical study and preclinical efficacy model, a desirable therapeutic target for further clinical studies would be steady-state trough concentrations that exceed 20  $\mu\text{g/mL}$ . In 1000 subjects bootstrapped from the original data set, the simulated serum pertuzumab-time profiles after a fixed, weight-based, or BSA-based dose were very similar. As expected, the use of the loading dose in the dosing regimens resulted in rapid attainment of steady-state concentrations within target concentration of 20  $\mu\text{g/mL}$  in the majority of patients. Weight-based or BSA-based dosing was found to decrease population variability of simulated steady-state trough serum concentrations on day 84 by only 6.2 and 5.8%, respectively, when compared to fixed dosing. In addition, the percentages of subjects with predicted steady-state trough serum concentrations below a selected target of 20  $\mu\text{g/mL}$  were low (<10%) and similar with all three dosing methods. Similar results were obtained from the subgroup analysis in population with extreme body weight (i.e.,  $\text{WT} \leq 10\text{th}$  and  $\geq 90\text{th}$  percentile). Hence, it is concluded that pertuzumab PK is related to WT and BSA. However, the WT and BSA explained only a small percentage of the interindividual variability of CL and Vc, and WT- and BSA-based dosing do not seem to improve the predictability of pertuzumab steady-state exposures. Unless better predictor variables for pertuzumab PK are identified, it is recommended to apply fixed-dosing regimens for pertuzumab in adult female cancer patients.

Historically, the dosing of drugs in oncology by weight- or BSA-based methods has largely resulted from its use in the extrapolation of drug doses used in preclinical animal studies to those considered safe as starting doses for phase I clinical trials in cancer patients (10). Recently, the scientific rationale for BSA-based dosing of anticancer drug was questioned. In a retrospective assessment of 33 anticancer drugs in 1650 patients, only 5 drugs were BSA-based dosing thought to be of clinical relevance (11). Recent PK analyses

of a number of small molecule oncology drugs typically dosed on BSA, such as topotecan (22), cisplatin (23), and irinotecan (24,25), have shown no rationale for BSA-based dosing of these agents in cancer patients.

To our knowledge, this is the first paper that reported a critical assessment of the impact of weight- or BSA-based dosing of a human IgG1 monoclonal antibody on steady-state drug concentrations in cancer patients. Implementation of flat-fixed dosing has several significant patient care and economic implications: (1) lower costs because of greater efficiency in manufacturing, storing, and shipping of single unit dose; (2) efficient preparation of a single dose in pharmacies and hospitals without the need for patient individualization; (3) greater efficiency in physician prescribing of single unit dose; and (4) lower likelihood of patient receiving wrong dose because of dose calculation errors (10). Although humanized antibodies are typically dosed by weight or BSA, our analyses demonstrate the feasibility of administering pertuzumab using a fixed dose in women with ovarian and breast cancers. Application to other populations such as males or to other IgG1 monoclonal antibody therapies will require further investigation.

## REFERENCES

1. D. Harari and Y. Yarden. Molecular mechanisms underlying ErbB2/HER2 action in breast cancer. *Oncogene* **19**:6102–6114 (2000).
2. Y. Yarden and M. X. Sliwkowski. Untangling the ErbB signalling network. *Nat. Rev. Mol. Cell Biol.* **2**:127–137 (2001).
3. M. X. Sliwkowski. Ready to partner. *Nat. Struct. Biol.* **10**:158–159 (2003).
4. H. S. Cho, K. Mason, K. X. Ramyar, A. M. Stanley, S. B. Gabelli, D. W. Denney Jr., and D. J. Leahy. Structure of the extracellular region of HER2 alone and in complex with the Herceptin Fab. *Nature* **421**:756–760 (2003).
5. D. B. Agus, R. W. Akita, W. D. Fox, G. D. Lewis, B. Higgins, P. I. Pisacane, J. A. Lofgren, C. Tindell, D. P. Evans, K. Maiese, H. I. Scher, and M. X. Sliwkowski. Targeting ligand-activated ErbB2 signaling inhibits breast and prostate tumor growth. *Cancer Cell* **2**:127–137 (2002).
6. C. L. Arteaga. ErbB-targeted therapeutic approaches in human cancer. *Exp. Cell Res.* **284**:122–130 (2003).
7. D. B. Agus, M. S. Gordon, C. Taylor, R. B. Natale, B. Karlan, D. S. Mendelson, M. F. Press, D. E. Allison, M. X. Sliwkowski, G. Lieberman, S. M. Kelsey, and G. Fyfe. Phase I clinical study of pertuzumab, a novel HER dimerization inhibitor, in patients with advanced cancer. *J. Clin. Oncol.* **23**:2534–2543 (2005).
8. D. E. Allison, M. A. Malik, F. Qureshi, D. Baker, S. Kelsey, G. Fyfe, M. Gordon, C. Taylor, and D. B. Agus. Pharmacokinetics of HER2-targeted rhuMAb 2C4 (pertuzumab) in patients with advanced solid malignancies: Phase Ia results. *Proc. Am. Soc. Clin. Oncol.* **22**:197 (2003).
9. J. F. Lu, S. Gourley, and R. Bruno. When should dose be adjusted to body size? A population pharmacokinetic (PPK) simulation. *Clin. Pharmacol. Ther.* **73**:86 (2003).
10. M. J. Egorin. Horseshoes, hand grenades, and body-surface area-based dosing: aiming for a target. *J. Clin. Oncol.* **21**:182–183 (2003).
11. S. D. Baker, J. Verweij, E. K. Rowinsky, R. C. Donehower, J. H. Schellens, L. B. Grochow, and A. Sparreboom. Role of body surface area in dosing of investigational anticancer agents in adults, 1991–2001. *J. Natl. Cancer Inst.* **94**:1883–1888 (2002).
12. A. Felici, J. Verweij, and A. Sparreboom. Dosing strategies for anticancer drugs: the good, the bad and body-surface area. *Eur. J. Cancer* **38**:1677–1684 (2002).
13. A. J. Boeckmann and S. L. Beal. *NONMEM User Guide, NONMEM Project Group*, University of California, San Francisco, 1994.
14. U. Wahlby, E. N. Jonsson, and M. O. Karlsson. Assessment of actual significance levels for covariate effects in NONMEM. *J. Pharmacokinetic. Pharmacodyn.* **28**:231–252 (2001).
15. Y. Yano, S. L. Beal, and L. B. Sheiner. Evaluating pharmacokinetic/pharmacodynamic models using the posterior predictive check. *J. Pharmacokinetic. Pharmacodyn.* **28**:171–192 (2001).
16. A. Gelman and X. L. Meng. Model checking and model improvement. In W. R. Gilks, S. Richardson, and D. J. Spiegelhalter (eds.), *Markov Chain Monte Carlo in Practice*, Chapman & Hall/CRC, Boca Raton, 1996, pp. 189–202.
17. A. Gelman, J. B. Carlin, H. S. Stern, and D. B. Rubin. *Bayesian Data Analysis*, Chapman & Hall/CRC, Boca Raton, 2004.
18. K. A. Harris, C. B. Washington, G. Lieberman, J. F. Lu, R. Mass, and R. Bruno. A population pharmacokinetic (PK) model for trastuzumab (Herceptin) and implications for clinical dosing. *Proc. Am. Soc. Clin. Oncol.* **21**:488a (2002).
19. B. Leyland-Jones, K. Gelmon, J. P. Ayoub, A. Arnold, S. Verma, R. Dias, and P. Ghahramani. Pharmacokinetics, safety, and efficacy of trastuzumab administered every three weeks in combination with paclitaxel. *J. Clin. Oncol.* **21**:3965–3971 (2003).
20. J. F. Lu, J. Gaudreault, W. Novotny, B. Lum, and R. Bruno. A population pharmacokinetic model for bevacizumab. *Clin. Pharmacol. Ther.* **75**:91 (2004).
21. M. A. Malik, K. Totpal, I. Balter, M. X. Sliwkowski, N. Pelltier, M. Reich, T. Crocker, S. Freiss, S. Bauer, N. H. Fiebig, and D. E. Allison. Dose-response studies of recombinant humanized monoclonal antibody 2C4 in tumor xenograft models. *Proc. Am. Soc. Cancer Res.* **44**:176–177 (2003).
22. W. J. Loos, H. Gelderblom, A. Sparreboom, J. Verweij, and M. J. Jongede. Inter- and inpatient variability in oral topotecan pharmacokinetics: implications for body-surface area dosage regimens. *Clin. Cancer Res.* **6**:2685–2689 (2000).
23. F. E. de Jongh, J. Verweij, W. J. Loos, R. de Wit, M. J. de Jonge, A. S. Planting, K. Nooter, G. Stoter, and A. Sparreboom. Body-surface area-based dosing does not increase accuracy of predicting cisplatin exposure. *J. Clin. Oncol.* **19**:3733–3739 (2001).
24. R. H. Mathijssen, J. Verweij, M. J. de Jonge, K. Nooter, G. Stoter, and A. Sparreboom. Impact of body-size measures on irinotecan clearance: alternative dosing recommendations. *J. Clin. Oncol.* **20**:81–87 (2002).
25. F. A. de Jong, R. H. Mathijssen, R. Xie, J. Verweij, and A. Sparreboom. Flat-fixed dosing of irinotecan: influence on pharmacokinetic and pharmacodynamic variability. *Clin. Cancer Res.* **10**:4068–4071 (2004).